

Design of Tiny High-Power Motor Driver without Liquid Cooling for Humanoid JAXON

Fumihito Sugai, Kunio Kojima, Yohei Kakiuchi, Kei Okada, and Masayuki Inaba

Abstract—In this paper, we present the design of a tiny high-power motor driver without a liquid cooling system. A high-power humanoid robot JAXON developed in our laboratory has a liquid cooling system for cooling motors and motor drivers. Thanks to the liquid cooling system, JAXON realizes high-power motion. However, the liquid cooling system makes the robot heavy. Hence, we designed a motor driver which is air cooling and smaller than the existing one while keeping its performance. There are two key points to realize tiny high-power motor driver. One is absorbing temperature rise due to instantaneous high current by using a heavy copper circuit board as a thermal buffer. The other is keeping steady board temperature low by reducing power consumption of motor driver. By applying developed motor driver to JAXON1, JAXON1 was able to reduce the weight of 7.1 [kg].

I. INTRODUCTION

A high-power humanoid robot JAXON (Fig. 1) has been developed in our laboratory as a platform for studying disaster response. An actuator system of JAXON is designed based on the actuator system by Urata et al. [1]. He realized a high power and high-speed motion with the humanoid robot by using the liquid cooling motor and motor driver. By using the liquid cooling system, a continuous current increases about twice. It enables JAXON realizing high power motion, such as climbing the 400 [mm] height step and squatting with holding 80 [kg] barbell in addition to JAXON's weight 127 [kg]. However, the weight of the liquid cooling system (3.8 [kg]; a detail of the liquid cooling system and motor driver are shown in Table I) makes JAXON heavy. It is concerned that increasing weight leads to decreasing kinematic performance, shortening battery life, and growing impact force of fall. Fig. 2 shows a configuration of motor drivers of JAXON. From this figure, it is shown that a large number of motor drivers occupy the volume of the robot hardware. Motor drivers for leg's motors are mounted inside the leg links. On the other hand, other motor drivers are put in backpack due to the convenience of placement pipes for the liquid cooling system. It increases a backpack size and structural material of a robot and makes JAXON heavy. Hence, we designed a smaller motor driver than the existing one while keeping JAXON's performance.

Several studies that focus on increasing actuator's performance by improving cooling performance have been done. Kim et al. use the liquid cooling system for cooling motors of series elastic actuators [2]. The weight of this liquid cooling system is approximately 1 [kg]. The motor driver

Authors are with Graduate School of Information Science and Technology, University of Tokyo, 7-3-1 Hongo, Bunkyo-ku, Tokyo 113-8656, Japan
sugai@jsk.imi.i.u-tokyo.ac.jp

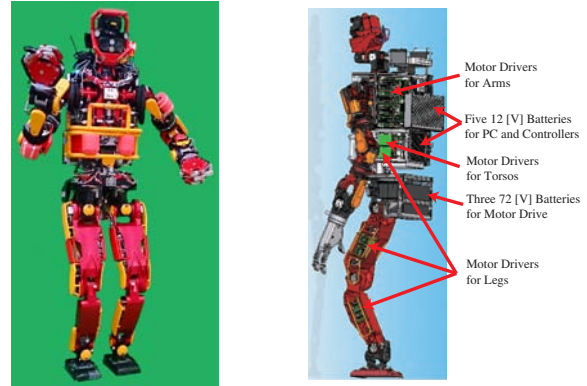


Fig. 1. Overview of JAXON. Fig. 2. Configuration of motor drivers.

is not cooled with the liquid cooling system. As a result, this actuator system can output 3.59 times larger continuous current than the system without liquid cooling. Lim et al. do not use the liquid cooling system but forced air cooling for cooling motors and motor drivers of humanoid robot DRC-HUBO+ [3]. This actuator system can output 1.7 times larger continuous current than the system without the air cooling system. Cooling motors with air cooling system can reduce the weight of cooling facilities, although the improving ratio of maximum continuous current becomes smaller. On the other hand, both methods do not use the liquid cooling system for cooling motor driver. However, in order to effectively utilize the maximum output performance of the motor, the motor driver is required to have higher output performance than the motor. Performance improvement due to cooling of the motor is more conspicuous in continuous output, and the peak output is very slight due to cooling performance. Therefore, in order to exert the peak output performance of the motor, larger peak output performance is required for the motor driver. In this research, we show that maximum peak performance can be improved without liquid cooling by novel design and improving power saving performance.

II. DEVELOPMENT OF TINY HIGH-POWER MOTOR DRIVER

Table II shows a weight of humanoid and a weight ratio of the motor driver. HRP-2 is a humanoid robot which has standard power actuator system. A weight ratio of the motor driver for JAXON is more than three times of HRP-2. A weight ratio of JAXON's motor driver includes the liquid cooling system. A weight ratio of the liquid cooling system is 3[%]. Hence, we designed a smaller motor driver than the



TABLE I

A BREAKOUT OF THE LIQUID COOLING SYSTEM AND MOTOR DRIVER.

Unit	Weight [g]	without new motor driver		with new motor driver	
		Qty.	Subtotal [g]	Qty.	Subtotal [g]
Pump	454	2	908	1	454
Radiator	360	2	720	1	360
Cooling fan	300	2	600	1	300
Liquid tank	205	2	410	1	205
Heat exchanger for motor driver	60	20	1200	6	360
Current motor driver (for low load)	158	19	3002	0	0
Current motor driver (for high load)	170	20	3400	12	2040
New motor driver	51	0	0	27	1377
Total			10240		5096

TABLE II

WEIGHT RATIO OF MOTOR DRIVERS.

	HRP-2	JAXON
		
DOFs	32	33
Weight [kg]	58	127
Weight ratio of motor driver [%]	1.9	7.1

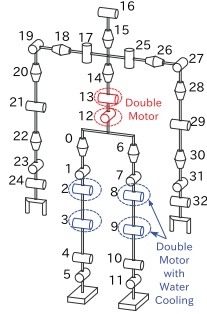


Fig. 3. Joint configuration of JAXON [4].

existing one while keeping JAXON's performance. At the same time, we designed it without liquid cooling, to increase the degree of freedom of placing the motor driver.

First of all, we clarified the required specification of the motor driver. Thinking about the performance of motor drivers, there are two evaluation indexes. One is the maximum current. If a maximum current is high, a robot can perform high power motion which uses instantaneous force such as jumping motion. The other is the continuous current. If the continuous current is high, a robot can do a task which needs high torque continuously such as carrying a heavy object. Therefore, we proposed two methods for a non-liquid cooling motor driver to make two evaluation indexes high. One is using a heavy copper circuit board as a thermal buffer. A heavy copper circuit board is used for mainly flowing high current. On the other hand, it has high heat capacity and acts as a thermal buffer to absorb the temperature rise caused by the high instantaneous current. It will make the maximum current of motor driver high. The other is low power consumption control methods. These methods reduce a heat value at steady state and make the temperature of motor driver low. It helps to make the continuous current of motor driver high.

A. Required Specification

Because the motor drivers for the lower limb are placed on the inside of the robot frame (Fig. 2), an effect of a

TABLE III

SPECIFICATION OF JAXON'S MOTOR DRIVER.

	for Low Load Part	for High Load Part
Voltage [V]	80	
Continuous Current [A]	50	
Maximum Current [A]	100	200
Size [mm]	85 × 60 × 34 (1-axis)	
	85 × 60 × 54 (2-axis)	
Weight [g] (including heat exchanger)	218	230

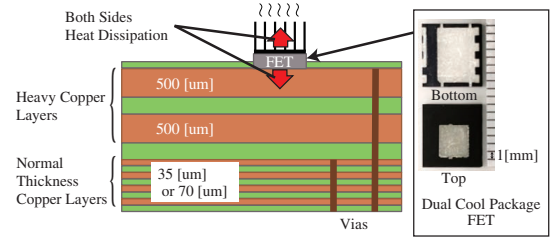


Fig. 4. Configuration of the circuit board's layers.

downsizing of the motor driver for the lower limb is limited. Therefore, we developed the motor driver for the upper limb. Table III shows a specification of the motor driver which JAXON currently uses. There are two kinds of motor driver depending on a load of each joint. Fig. 3 shows a joint configuration of JAXON. Motors of knee joints and hip-pitch joints are cooled with a liquid cooling system. Urata et al. identified a limit current of the same motor used by JAXON [1]. The motor is DC brushless motor EC-powermax 4 pole 200 [W] made by MAXON. A limitation continuous current of the liquid cooling motor and the non-liquid cooling motor is 20 [A] and 15 [A], respectively. A reduction gear of each joint is harmonic gear. Its maximum ratcheting torque, which is the limit value of torque transmission, is 1000 [Nm] for liquid cooling joint and 980 [Nm] for a non-liquid cooling joint. It becomes 136 [A] and 85 [A], respectively in motor current. From the above discussion, the specification of the motor driver for replacing original motor driver is as follow:

- Continuous current is greater or equal 15 [A].
- Maximum current is greater or equal 85 [A].
- Taking weight saving and handling of the piping of the liquid cooling system, the cooling method is forced air cooling.
- Size of motor driver is half of the existing one.

B. Design of tiny high-power motor driver

There are two difficult points to make motor drivers small. One is the heat dissipation problem because the heat source is concentrated. The other is hard to keep a trace width of the circuit board for high current flow. As a solution, we use a Dual Cool package FET (FDMT800100DC) made by Fairchild which is Surface Mount Device package and can heat away from both top side and bottom side as shown in Fig. 4. We choose a heavy copper circuit board that maximum thickness of copper is 0.5 [mm] to flow a high

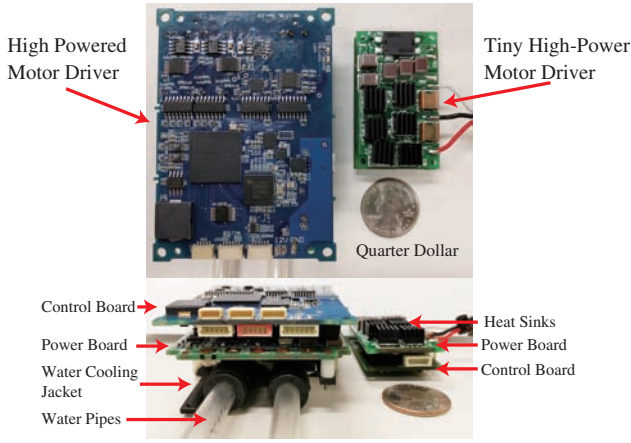


Fig. 5. Comparison between the high powered motor driver and tiny high-power motor driver.

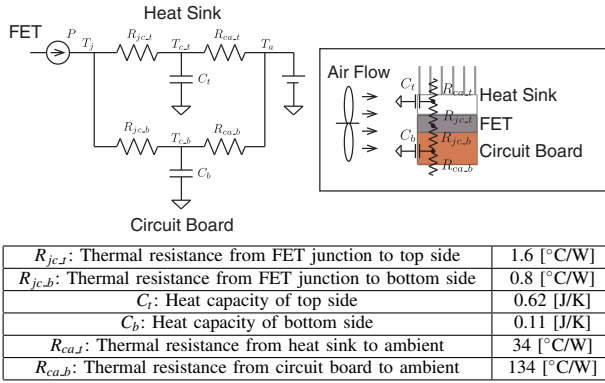


Fig. 6. Thermal model of FET to ambient and thermal parameters.

current. Fig. 4 shows a configuration of circuit board layers. Heavy copper layers are used as a trace of motor currents, and normal thickness copper layers are used as a trace of control signals.

Fig. 5 shows a comparison of high powered motor driver used in JAXON and tiny high-power motor driver we developed. A developed motor driver is less than a fifth of volume and less than a fourth of weight of former one. As shown in the figure, the tiny high-power motor driver consists of two circuit board; control board and power board. The control board has FPGA (Field Programmable Gate Array) Cyclone V(5CEBA4F17C8N) made by Intel. FPGA controls the motor current and communicates with a controller PC. In FPGA, there is a 32-bit softcore processor NIOS II. NIOS II runs tasks; position control, motor temperature estimation, and error protection.

To evaluate the performance of the developed motor driver, we built a thermal model of the motor driver and identified a thermal parameter. Firstly, we command the motor driver reference current. Then we measure the temperature of the circuit board of the motor driver. Fig. 7 shows a temperature distribution of the surface of the power board. Table V shows the board temperature for each reference current. From this

TABLE IV
SPECIFICATION OF THE TINY HIGH POWERED MOTOR DRIVER.

Voltage [V]	80
Continuous Current [A]	45
Maximum Current [A]	139
Size [mm]	54 × 32 × 20.5
Weight [g]	45
Interfaces	RS-485×2, RS-422×1, USB 2.0 Hi-Speed×1, GPIO×13, DIP-SW×8, Buzzer, JTAG

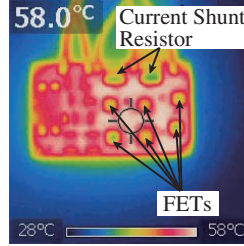


Fig. 7. Temperature distribution of circuit board.

TABLE V
BOARD TEMPERATURE AT EACH REFERENCE CURRENT.

Ref. Current [A]	Board Temperature [°C]
5	43.1
10	45.7
15	50.3

experimental result, we made a thermal model from FET to ambient and identified thermal parameters shown in Fig. 6. From this model, we can estimate a continuous current and maximum current as shown in Table IV. We defined continuous current as the current which does not heat FET's junction temperature (inside temperature of FET) more than 90°C. We also defined a maximum current as the current which does not exceed FET's junction temperature of FET over 120°C in 0.5 [s] when initial junction temperature of FET is 90°C. From Table IV, it is shown that the developed motor driver satisfies the required specification.

C. Using Heavy Copper Circuit Board as Thermal Buffer

By using a heavy copper circuit board as a thermal buffer, maximum current of the motor driver could be enlarged. The reason why the maximum current becomes high is that the heat capacity of the circuit board can make thermal time constant small. In other words, the thermal buffer can conduct heat away from FET to thermal buffer quickly. From thermal parameters shown in Fig. 6, thermal resistance of FET's bottom side $R_{jc,b}$ is smaller than FET's top side $R_{jc,t}$. Hence, adding the thermal buffer on the bottom side of FET is more effective than adding on the top side.

Fig. 8 shows a simulation result of the thermal model of the motor driver. As an initial condition, a motor driver outputs continuous current 45 [A], and temperature at each point is steady state. Then, the motor driver outputs maximum current 139 [A]. In Fig. 8, a temperature in the solid line shows the simulation result with the designed motor driver. Fig. 8 shows that the junction temperature of FET becomes 120 [°C] at 0.5 [s]. To establish the effectiveness adding the thermal buffer on the bottom side of FET, we simulate with moving half heat capacity of the circuit board to top side. The simulation result is shown dot-line in Fig. 8. From the simulation result, the junction temperature of FET exceeds

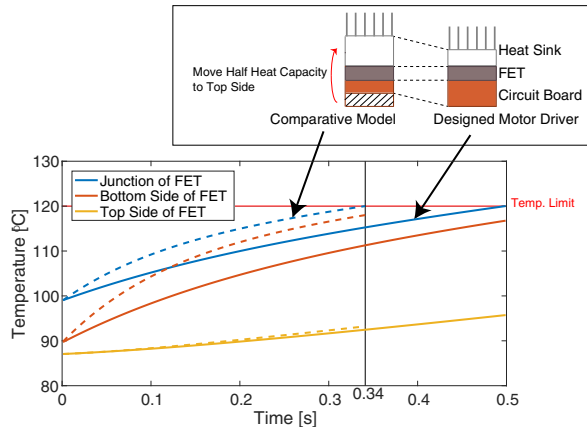


Fig. 8. Thermal response simulation to establish the effectiveness of the thermal buffer.

120 [°C] at 0.34 [s]. With this condition, a maximum current which does not exceed FET's junction temperature of FET over 120°C in 0.5 [s] becomes 103 [A]. From this simulation result, it is shown that the using heavy copper circuit board as the thermal buffer is useful for not only flowing high current but also increase maximum current.

Recently, a small high-power motor driver is now commercially available. The mobile platform of Rollin'Justin developed by DLR [5] and humanoid robot CHMIP developed by Carnegie Mellon University [6] use motor driver made by Elmo. Gold Twitter R80/80 made by Elmo (size: 35x30x14.4 [mm], weight: 22.2 [g]) can output 80 [A] current continuously. However, this specification is guaranteed when the temperature of a heat sink is 85 [°C]. Simulating with this condition, our motor driver could output 85 [A] continuously. On the other hand, an amount of pulsed current output is limited by the initial temperature of the motor driver. If the motor driver outputs low continuous current, motor driver will be able to output high pulsed current. Fig. 9 shows a relationship between the output possible time of pulsed current and initial continuous current. For instance, if the motor driver outputs 25 [A] continuously, it will be able to output about 200 [A] pulsed current for 0.5 [s]. If a continuous current is 5 [A], the motor driver can output about 220 [A] pulsed current for 0.5 [s]. As a result, low continuous current could make peak performance high.

As an example, we carried out a high-speed motion test. Fig. 10 shows an experimental setup. As a reduction gear, timing belt and harmonic gear are used. The length of the link is 0.5 [m]. As a load, 10 [kg] weight is attached to the link end. In the experiment, we set initial pose that link is downward as shown in Fig. 10. We send a reference trajectory, from 0 [s] to 0.5 [s] moving the link to be a horizontal pose, from 0.5 [s] to 4.5 [s] moving back to initial pose. Fig. 11 shows an experimental result. At 0.15 [s], a peak current; 65 [A] flowed into the motor. From 0.5 [s] to 4.5 [s], a current is about 10 [A]. From Fig. 9, 0.5 [s] output possible peak current becomes 216 [A] when continuous current is 10 [A]. As a result, it is confirmed that the motor

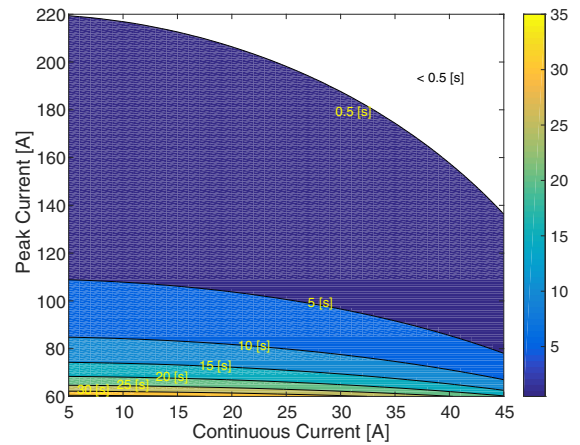


Fig. 9. Relationship between output possible time of pulsed current and initial continuous current.

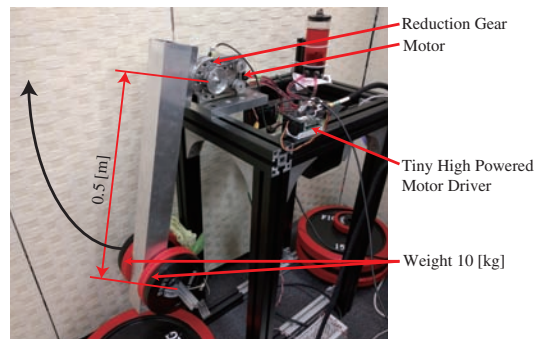


Fig. 10. Experimental setup for high speed motion.

driver could perform this high-speed motion again and again.

D. Low Power Consumption Control

The electrical power consumption of motor drivers can be divided into a power consumption for generating torque, conduction loss, and switching loss. These power losses of the motor driver have no effect of generating torque. Furthermore, these power losses make continuous current high and output possible time of pulsed current becomes low. Hence, we propose two methods which make motor driver low power consumption by reducing those losses.

1) *Dynamic Switching Frequency Control*: It is known that a switching loss is proportional to a switching frequency [7]. A switching frequency is determined by a maximum rotational speed of the motor. Hence, the robot which moves at high speed uses a motor driver whose switching frequency is higher than one of the commonly-used motor driver. For instance, Terasawa et al. executed swing motion of tennis by JAXON [8]. Because its motion is a high-speed motion, a switching frequency of the arm's motor driver was 39 [kHz]. Therefore, it causes a high loss constantly regardless of whether or not motor moves at high speed. Hence, we propose a control method which can reduce the switching loss to a minimum by dynamically controlling the switching frequency depending on the motor's rotational speed.

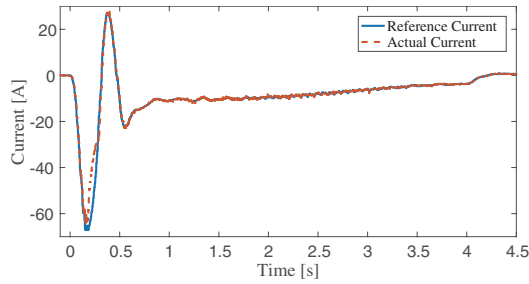


Fig. 11. Experimental result of high speed motion.

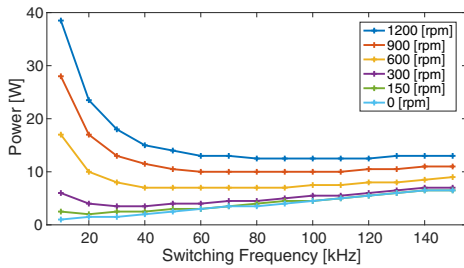


Fig. 12. Relationship between energy consumption and switching frequency.

There are previous works controlling switching frequency dynamically. Kishimoto proposed the method for railway inverter to change its switching frequency at unsynchronized PWM mode to reduce sound noise [9]. Okubo et al. proposed a control method for an electric vehicle's inverter to decrease a switching loss [10]. They change a switching frequency discretely depend on motor rotational speed in three level. However, there is no study to decrease switching loss by changing the switching frequency for the robot's motor driver. We propose a method to reduce switching loss by changing the switching frequency in proportion to motor rotational speed.

Firstly, we carried out an experiment to clarify an effect of a switching frequency on switching loss. A reference rotational speed of motor is 0, 150, 300, 600, 900, and 1200 [rpm]. A switching frequency is changed from 10 [kHz] to 150 [kHz] in 10 [kHz] increments. Fig. 12 shows an experimental result. From the result at 0 [rpm], it is confirmed that a switching loss is proportional to a switching frequency. It can be seen that as the rotation speed is increased, the switching frequency which the power consumption is minimum becomes higher. From this experimental result, it is shown that a switching loss can be minimized by controlling switching frequency depends on rotational speed.

Fig. 13 shows a block diagram of the motor driver. We add a Switching Frequency Controller and modify a PWM Generator to change switching frequency dynamically. In Position Controller, it calculates reference rotational speed and optimal switching frequency from a reference position and sends it to Switching Frequency Controller. Switching Frequency Controller sends a reference frequency to PWM Generator. PWM Generator changes its output frequency in synchronization with the switching cycle.

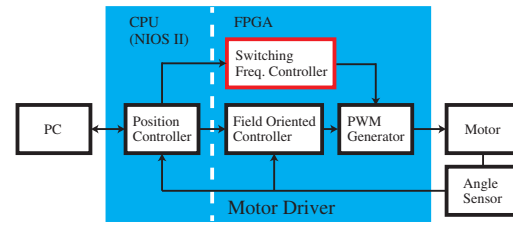


Fig. 13. Block diagram of the motor driver.

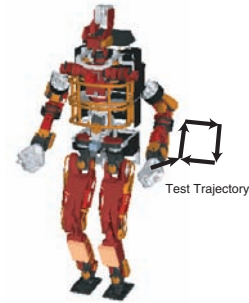


Fig. 14. Initial pose of JAXON and test trajectory.

2) *Automated Switching Sleep Control*: By applying dynamic switching frequency control proposed in above, a switching loss could be minimized. However, it is not possible to set switching frequency lower than the frequency which is determined by an electrical time constant. Hence, dynamic switching frequency control is not sufficient for a joint axis which is stopping.

In the meantime, thinking about task execution by the humanoid, it is few cases that all joints keep moving. At the DARPA Robotic Challenge; competition of disaster response robot, JAXON executed following tasks: drive a vehicle, egress from the car, open a door, open a valve, cut a wall, traverse rubble, climb stairs, and so on [11]. During one-hour task operation time, JAXON spent 26 minutes to wait for a command from an operator or walk to next task place. Therefore, the time to perform the manipulation task is a short time. In other times it was in a state where the joint angle was kept constant except for the leg which is performing the balance control. Therefore, we propose a control method that realizes low power consumption by cutting off the motor output that does not move the joint.

As related work to reduce power consumption of joint on standby, Toda et al. use an electromagnetic brake to hold the posture of the arm without motor output [12]. Meike et al. studied energy efficiency for the industrial robot in the automobile industry. They discuss the effective use of an electromagnetic brake when robot arms are standby state [13]. However, adding a brake mechanism leads to make robot heavy. For instance, if electromagnetic brakes whose brake torque is 0.1 [Nm] same as maximum torque of motor are mounted on all JAXON's arm joint, it causes 0.5 [kg] weight increase. Hirzinger et al. developed a lightweight brake using a piezoceramic element [14]. Although its weight

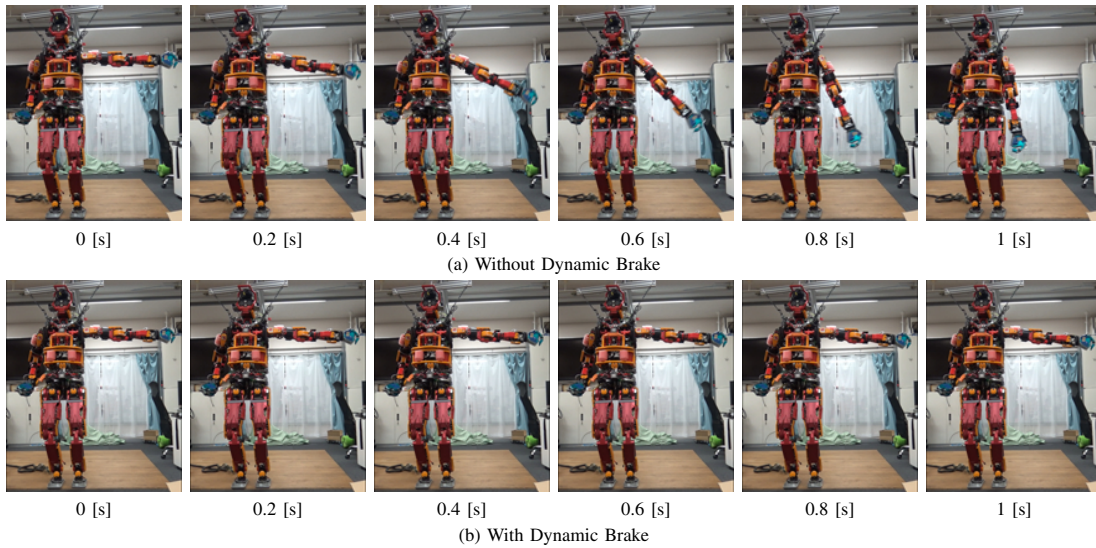


Fig. 15. Effect of dynamic brake at a left shoulder pitch joint.

TABLE VI

TORQUE CURRENT OF JAXON'S LEFT ARM AT THE INITIAL POSE.

Joint (No.)	Current [A]	Output Axis Torque [Nm]
Collar yaw (25)	0.058	0.55
Shoulder pitch (26)	0.58	5.5
Shoulder roll (27)	1.0	9.7
Shoulder yaw (28)	0.16	1.6
Elbow pitch (29)	1.1	11
Wrist yaw (30)	0.0039	0.037
Wrist roll (31)	0.11	1.1
Wrist pitch (32)	0.25	2.4

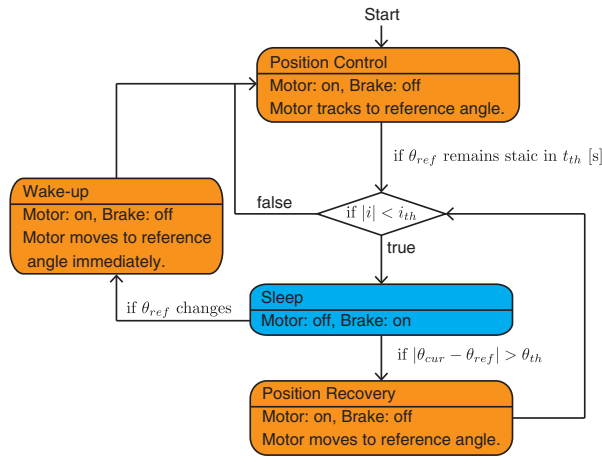


Fig. 16. A state machine of automated switching sleep control.

is half of the existing one, it cannot keep away weight increase.

When a robot does not execute manipulation tasks, an accuracy of end-effector position is not needed. However, cutting off motor output and making joint freely rotate is not good because it causes self-collision or colliding with an environment. Therefore, by using mechanical friction on the joint axis and dynamic braking of the motor, we reduce power consumption without adding any new device.

JAXON's arm joint uses harmonic drive gear CSD20-160 (gear ratio 160:1). Its backdriving torque, which is a torque starting rotate from the output axis, is 6.6 [Nm]. In fact, the joint axis whose load torque is 6.6 [Nm] below can keep its joint angle although motor output torque becomes zero. Fig. 14 shows an initial pose of JAXON. Table VI shows a measured motor output current and joint torque converted from the output current at the initial pose. At initial pose, the output axis torque of 5 joints out of 8 joints is lower than 6.6 [Nm] and can keep its angle without motor output. However, disturbance torque could change arm posture easily if motor output torque is zero. Hence we use a dynamic brake as a resistance torque. A dynamic brake is a brake which comes of returning current from a back electromotive force by shorting the motor circuit. Since a dynamic brake function could be realized by only changing its software, it is not required to add any hardware.

We evaluate the braking torque of the dynamic brake. An output torque of motor τ_m is derived as follow:

$$\tau_m = K_t i, \quad (1)$$

where K_t is a torque constant; i is a current. A terminal voltage V_m is derived as follow:

$$V_m = R_e i - \frac{\omega}{K_e}, \quad (2)$$

where R_e is a terminal resistance; ω is a rotational speed of the motor; K_e is a speed constant, respectively. When a dynamic brake is enabled, wires of a motor are shorted; $V_m = 0$. Hence braking torque τ_b can be derived by the following equations:

$$\tau_b = K_b \omega = \frac{K_t}{K_e R_e} \omega = \frac{K_t^2}{R_e} \omega. \quad (3)$$

From the above equations, it is shown that the braking force is proportional to rotational speed. JAXON uses a brushless DC motor (EC-4pole 30 200W (305014)) made by MAXON. From Equation (3) and parameters of motor,

K_b is 0.002 [Nm/(rad/s)]. By considering gear ration of arm 460.8, K_b is 0.92 [Nm/(rad/s)] on joint axis.

To measure the effect of the dynamic braking, we conducted an experiment. Fig. 15 shows an experimental result. The initial pose of the left arm is horizontally fully-stretched, then we turn off the power of a shoulder-pitch joint. We compared between just making motor output zero or using the dynamic brake. In the case where a dynamic brake is not used, the arm is falling in 1 [s]. On the other hand, it took 33 [s] in the case of using the dynamic brake. From this result, a dynamic brake functions effectively as a resistance force on a joint axis.

From the above discussion, we propose a strategy for reducing power consumption as shown in Fig. 16. In Position Control state, motor tracks to the reference angle. If a reference angle θ_{ref} does not change for a time t_{th} and motor output current i is smaller than threshold value i_{th} , motor driver state changes to the Sleep state. In Sleep state, the motor driver cuts off output and enables dynamic brake. If an error angle between reference angle θ_{ref} and the current angle θ_{cur} becomes larger than the threshold angle θ_{th} , motor driver state changes to Position Recovery state. In Position Recovery state, the motor driver moves the motor to the reference angle. If a reference angle θ_{ref} changes, motor driver state changes to Wake-up state. In Wake-up state, the motor driver moves the motor to the reference angle immediately.

There are three parameters; θ_{th} , t_{th} , i_{th} in this strategy. t_{th} does not affect reducing the amount of power consumption and is set to 2 [s]. θ_{th} is a threshold value of how much angle change is allowed on the motor axis and is set to $\pi/2$. This value is set to make the position variation of end-effector smaller than 5 [mm] in JAXON's arm. Power consumption will decrease if the reduction of the motor driver's power loss is larger than lost kinetic energy due to cutting off motor output. Therefore, if the load torque τ_l satisfies the following equation, power consumption will decrease.

$$\tau_l \theta_{th} / N < P_{loss} t_s, \quad (4)$$

where N is a gear ratio, P_{loss} is a power of switching loss, and t_s is a time in the Sleep state, respectively. t_s is calculated by following equation of motion.

$$\begin{cases} I \ddot{\theta}(t) = \tau_l - D \dot{\theta}(t) \\ \theta(t_s) = \theta_{th} / N \end{cases}, \quad (5)$$

where I is inertia of joint axis, θ is the angle of the joint axis, D is viscosity resistance of joint axis, respectively. Because of rotation angle θ_{th} / N is small, we treat τ_l as constant. D is a summation of viscosity resistance of harmonic gear and dynamic braking torque. D is estimated by the experimental result. From the above equations, the threshold load torque τ_l was derived as 20 [Nm].

3) *Evaluation Test*: We experimented to evaluate the effect of two proposed methods. We applied proposed methods to joints of arms and head. JAXON moves the left arm with the certain trajectory in 5 [s] and rests 5 [s] shown in Fig. 14 Left arm moves along reference trajectories in 0 [s]

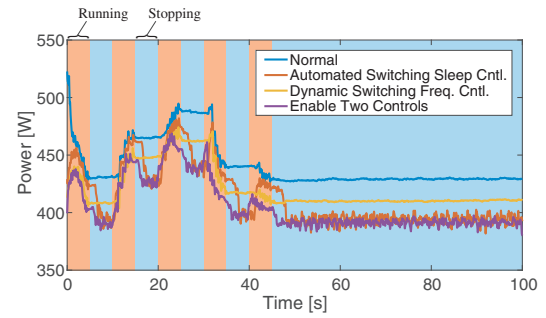


Fig. 17. Power consumption of JAXON's whole motor driver.

TABLE VII
POWER CONSUMPTION.

Method	Power [W]
Normal	442
Automated Switching Sleep Control	413
Dynamic Switching Frequency Control	421
Enable Both Two Methods	405

to 50 [s] then rests 50 [s]. The whole power consumption of JAXON was measured. The experiment was conducted in four conditions; without any additional control, with dynamic switching frequency control, with automated switching sleep control, with two proposed controls.

Fig. 17 shows an experimental result. From 0 [s] to 50 [s], the arm is moving. From 50 [s] to 100 [s], JAXON keeps its posture. In Fig. 17, colored in red indicates moving and colored in blue indicates resting. By applying either method, power consumption becomes lower than the one without using any method. In the case of dynamic switching frequency control, power consumption becomes a power consumption without using any method minus a certain amount. In the case with automated switching sleep control, power consumption decreases after a certain period has elapsed since JAXON stopped moving. In the case of applying both methods, power consumption is the lowest of the four conditions.

Table VII shows average power consumption in four cases. An effect of reducing power consumption depends on the ratio of standby time to working time. If the ratio of the task executing time to operating time is 50%, the proposed method can reduce 37 [W]. Thanks to this reduction of power consumption, JAXON could reduce one battery which is 2 [kg] weight while maintaining the operating time.

III. APPLYING DEVELOPED MOTOR DRIVER TO JAXON

We applied developed tiny high-power motor driver to JAXON1 (we have two JAXONs almost same configuration). We replaced 27 motor drivers of upper limb joints of JAXON1. In Table I shows the comparison about the liquid cooling system and motor drivers between before and after applying the tiny high-power motor driver. By replacing 27 motor drivers, we could reduce a 3 [kg] weight from JAXON1. By applying tiny high-power motor driver, JAXON1 becomes low power consumption. Hence, JAXON1



Fig. 18. Comparison backpack of JAXON1 before and after applying the tiny high-power motor driver.

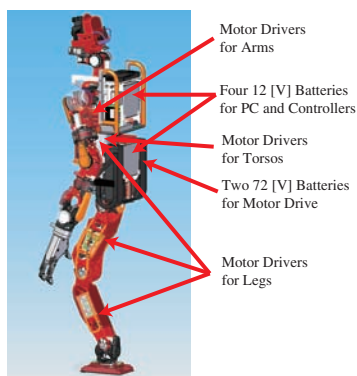


Fig. 19. JAXON2 optimized for the tiny high-power motor driver.

could reduce one battery (weight is 2 [kg]) despite keeping its operating time. By replacing the motor driver with liquid cooling to tiny high-power motor driver without liquid cooling, JAXON1 could reduce the liquid cooling system to half. By applying developed motor driver, total weight reduction of JAXON1 is 7.1 [kg].

Fig. 18 shows a comparison backpack before and after applying the tiny high-power motor driver to JAXON1. In Fig. 18, a dotted line shows a region of the motor drivers. From this figure, it is shown that tiny high-power motor driver could make backpack small. Hence, we improve the design of JAXON2 for the tiny high-power motor driver. Fig. 19 shows the optimized design of JAXON2 for the tiny high-power motor driver. Thanks to miniaturization of the motor driver, the motor driver could be placed in a torso link. As a result, a backpack size will be small. The assumption of the weight reduction is 10 [kg].

After applying tiny high-power motor driver, JAXON1 performs many tasks such as tennis swing motion [8], soil-digging tasks [15]. These tasks require high speed and high torque motion. JAXON1 with the tiny high-power motor could perform these task as before change of motor driver.

IV. CONCLUSIONS

In this paper, we showed the design of tiny high-power motor driver without liquid cooling for humanoid robot JAXON. We described the weight ratio of the motor driver and the liquid cooling system is high, and it makes the robot heavy. Then we developed the tiny high-power motor driver which maintains its performance. We proposed two methods for realizing high-power motor driver within a small size. One is using a heavy copper circuit board as a thermal buffer to make maximum current high. The other is low power consumption controls to make continuous current high. As a result, we realized the motor driver which is small and lightweight, cooling with air cooling, and low power consumption. By using developed motor driver, we successfully reduce humanoid robot JAXON's weight minus 7.1 [kg] (motor driver 3 [kg], battery 2 [kg], liquid cooling system 2.1 [kg]). In the future work, we will improve the liquid cooling motor driver for lower limb and reduce the JAXON's weight under 100 [kg] while keeping its performance.

REFERENCES

- [1] J. Urata, et al., "Design of high torque and high speed leg module for high power humanoid," in *Proceeding of 2010 IEEE/RSJ International Conference on Intelligent Robots and Systems (IROS)*, 2010.
- [2] D. Kim, et al., "Investigations of a Robotic Testbed with Viscoelastic Liquid Cooled Actuators." in arXiv:1711.01649v2 [cs.SY], 2018
- [3] J. Lim, et al. "Robot System of DRC-HUBO+ and Control Strategy of Team KAIST in DARPA Robotics Challenge Finals." in *Journal of Field Robotics*, vol. 34, no. 4, pp. 802–829, 2017.
- [4] K. Kojima, et al., "Development of life-sized high-power humanoid robot jaxon for real-world use," in *Proceeding of IEEE-RAS 15th International Conference on Humanoid Robots (Humanoids)*, 2015.
- [5] M. Fuchs, et al. "Rollin'Justin-Design considerations and realization of a mobile platform for a humanoid upper body." in *Proceeding of IEEE International Conference on Robotics and Automation*, 2009.
- [6] A. Stentz, et al. "Chimp, the cmu highly intelligent mobile platform." in *Journal of Field Robotics*, vol. 32, no. 2, pp. 209-228, 2015.
- [7] P. Matthias, et al. "Switching Frequency Reduction Using Model Predictive Direct Current Control for High-Power Voltage Source Inverters." in *IEEE Transactions on Industrial Electronics*, vol. 58, issue 7, 2011.
- [8] R. Terasawa, et al., "Achievement of dynamic tennis swing motion by offline motion planning and online trajectory modification based on optimization with a humanoid robot." in *Proceeding of IEEE-RAS 16th International Conference on Humanoid Robots (Humanoids)*, 2016.
- [9] T. Kishimoto, "Noise Caused by Propulsion System of Electric Rolling Stock", in *Noise Control*, vol. 29, no. 4, pp. 287–289, 2005. (in Japanese)
- [10] K. Okubo et al. "Development of the inverter to decrease loss for electric vehicle (EV) motor", in *Mitsubishi Heavy Industries, Ltd. Technical Review*, vol. 45, no. 3, 2008.
- [11] Y. Kakiuchi, et al. "Development of humanoid robot system for disaster response through team nedo-jsk's approach to darpa robotics challenge finals." in *Proceeding of IEEE-RAS 15th International Conference on Humanoid Robots (Humanoids)*, 2015.
- [12] K. Toda, et al. "Camera arm system for disaster response robots." in *Proceeding of International Conference on Design Engineering and Science*, pp.80–85, 2014.
- [13] D. Meike, et al. "Energy efficient use of robotics in the automobile industry." in *Proceeding of 15th International Conference on Advanced Robotics (ICAR)*, 2011.
- [14] G. Hirzinger, et al. "Advances in robotics: the DLR experience." in *The International Journal of Robotics Research*, vol. 18, no. 11, pp. 1064–1087, 1999.
- [15] S. Komatsu, et al. "Tool Force Adaptation in Soil-Digging Task for Humanoid Robot." in *Proceeding of IEEE-RAS 16th International Conference on Humanoid Robots (Humanoids)*, 2016.